ChemComm

COMMUNICATION

View Article Online
View Journal | View Issue

Cite this: *Chem. Commun.*, 2019, **55**, 13426

Received 13th August 2019,
Accepted 14th October 2019

DOI: 10.1039/c9cc06200a

rsc.li/chemcomm

Type III-C rotaxane dendrimers: synthesis, dual size modulation and *in vivo* evaluation†

Chak-Shing Kwan,‡[a] Tao Wang,‡[a] Min Li,[b] Albert S. C. Chan,[c] Zongwei Cai *[a] and Ken Cham-Fai Leung *[a]

Type III-C rotaxane dendrimers were synthesized by a divergent approach. Dual shuttling behavior and size modulation were observed from non-methylated/methylated rotaxane dendrimers under the same external stimuli. The biological distribution of dendrimers in C57BL/6J mice determined by MALDI-TOF-MS shows predominant accumulation in the spleen and liver. Drug encapsulations with chlorambucil and lithocholic acid were demonstrated.

Rotaxane dendrimers (RDs) are a class of mechanically interlocked molecules (MIMs) combining the unique linear molecular shuttling properties and motif of mechanically interlocking systems into spherical dendrimers to generate hyperbranched mechanically interlocked macromolecules. The concept of rotaxane dendrimers was first defined by Lee and Kim[1] in 2003 and further elaborated by Stoddart *et al.* in 2017.[2] It is classified into three main RD types (I, II and III) and each type can be further divided into sub-categories (A, B, and C). Among those, the synthesis of type III rotaxane dendrimers is the most challenging task, as they have a dendritic polyrotaxane architecture with interlocking moieties from the core to every branching unit. Equipped with three-dimensional, near-spherical macromolecular structures as well as the collective molecular shuttling properties of type III rotaxane dendrimers,[3] it is believed that they could potentially be utilized in various applications such as catalysis,[4] drug delivery, molecular electronics, *etc.*, controlled by different external stimuli, such as pH,[5] light radiation,[6] redox,[7,8] *etc.* Our group has recently reported the first successful synthesis of high-generation type III-B G3 rotaxane dendrimers and a G4 dendron with three-dimensional switching and demonstrated their applicability in drug encapsulation.[9] Due to the complexity of the structures and the difficulties in chemical synthesis, only a few examples of type III RDs have been successfully reported[9–13] and their switching properties have been demonstrated.[9,13]

Type III-C rotaxane dendrimers were first categorized by Stoddart *et al.* in 2017,[2] as the branches extend from the rings rather than the rods. In particular, type III-C RDs have mechanical bonds in between and constituted the branching points. Only one example that matches the description of type III-C RDs was reported by Liu *et al.* in 2013,[14] as the first-generation (**G1**) hetero[4]rotaxane. However, their strategy failed to produce higher generation RDs because of the non-functionalized macrocycle.

We envisage a divergent approach toward the chemical synthesis of type III-C rotaxane dendrimers (Scheme 1). Similar to the traditional dendrimer synthesis,[15] the branching unit grows outward from the core [2]rotaxane to become a hyperbranched rotaxane dendrimer.

The stimuli-responsive molecular shuttling properties and globular structures of type III-C RDs could be potentially applied in drug encapsulation and a pH responsive delivery system.[9] The biological distribution of these potential cargo carriers is crucial to achieve localized and targeted delivery. Conventionally, the *in vivo* study of dendrimers usually relies on a radiolabel or fluorescence label covalently attached to dendrimers. Matrix assisted laser desorption-time of flight mass spectrometry (MALDI-TOF MS) could be a versatile tool for us to analyze

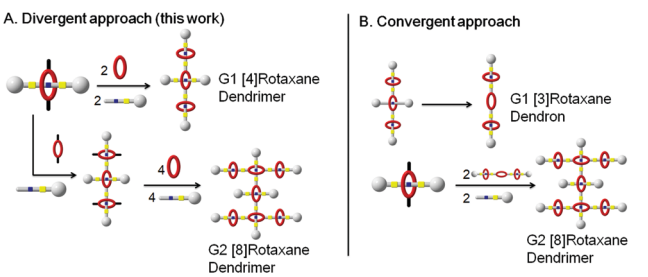

Scheme 1 Proposed divergent (A) and convergent (B) approaches towards the synthesis of type III-C RDs.

[a] *Department of Chemistry and State Key Laboratory of Environmental and Biological Analysis, Hong Kong Baptist University, Kowloon Tong, Kowloon, Hong Kong SAR, P. R. China. E-mail: cfleung@hkbu.edu.hk, zwcai@hkbu.edu.hk*
[b] *School of Chinese Medicine, Hong Kong Baptist University, Kowloon Tong, Kowloon, Hong Kong SAR, P. R. China*
[c] *School of Pharmaceutical Sciences, Sun Yat-sen University, Guangzhou, P. R. China*

† Electronic supplementary information (ESI) available: Experimental, NMR spectra, shuttling process, *in vivo* study, *etc.* See DOI: 10.1039/c9cc06200a

‡ These authors contributed equally.

label-free type III-C RDs *in vivo*. To broaden the scope of rotaxane dendrimers, herein we present a facile divergent synthesis of type III-C rotaxane dendrimers equipped with dual shuttling functions for size modulation. The binding of two drug molecules (chlorambucil and lithocholic acid) has been studied. *In vivo* biological distributions of the label-free MIMs by MALDI-TOF MS were also investigated. To the best of our knowledge, it is the first rotaxane dendrimer that possesses dual (expansion and contraction) collective size modulation for drug encapsulation.

The key-precursor in type III-C RD synthesis is the di-functionalized crown ether in the first step of [2]rotaxane formation. Di-succinimide (NHS) functionalized [2]rotaxane (**2-H·PF$_6$**) was synthesized in about 67% yield (the detailed synthetic route is illustrated in the ESI†). The NHS moiety was transformed to an azide moiety (**3-H·PF$_6$**) followed by the formation of two new mechanical bonds through ubiquitous copper catalyzed azide alkyne cycloaddition (CuAAC), giving **G1** [4]rotaxane dendrimer (**G1-H$_3$·3PF$_6$**) in 63% yield. A tetra-functionalized-NHS **G1** [4]rotaxane dendrimer (**4-H$_3$·3PF$_6$**) was synthesized by replacing DB24C8 with di-functionalized DB24C8 in the first step. The four NHS units on **4-H$_3$·3PF$_6$** were transformed to azide ended tetra-functionalized **G1** [4]rotaxane dendrimer (**5-H$_3$·3PF$_6$**) and used in the formation of **G2** [8]rotaxane dendrimer (**G2-H$_7$·7PF$_6$**). The synthesis of **G2-H$_7$·7PF$_6$** involved the formation of four new mechanical bonds in one step CuAAC. Encouragingly, we were able to isolate the final pure **G2-H$_7$·7PF$_6$** in 56% yield. Triazole methylation of **G1-H$_3$·3PF$_6$** and **G2-H$_7$·7PF$_6$** was performed for the further investigation on switching (Fig. 1).

All type III-C RDs were well characterized thoroughly by ^{1}H and ^{13}C NMR spectroscopies. The starting [2]rotaxane was characterized by ^{1}H NMR with two NHS moieties in di-NHS [2]rotaxane (**2-H·PF$_6$**). When it was transformed into di-azido [2]rotaxane (**3-H·PF$_6$**), the original succinimide proton peak at δ = 2.76 ppm was transformed into two sets of new peaks at δ = 4.27 ppm, and δ = 4.45 ppm corresponding to the azide moiety (Fig. S5, ESI†).

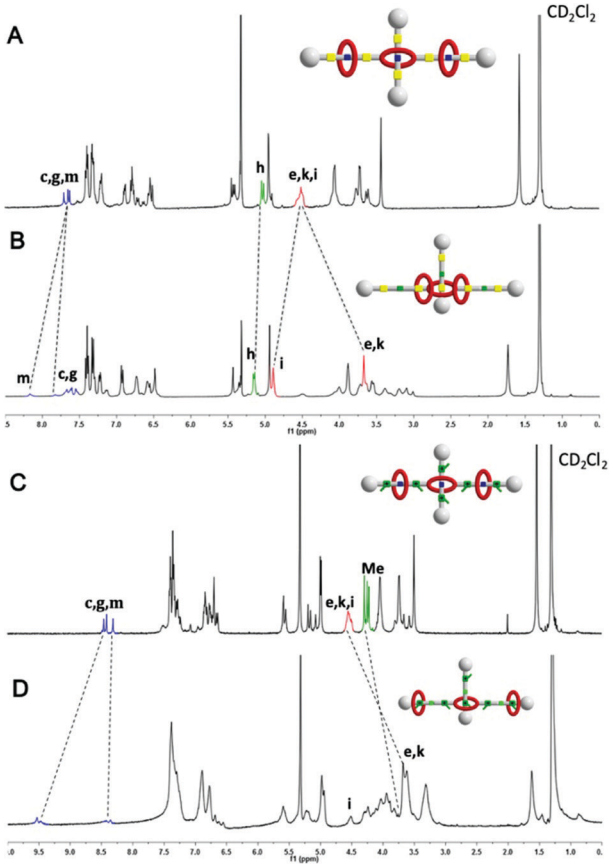

Fig. 2 Stacked ^{1}H NMR spectra (400 MHz, CD_2Cl_2, 298 K) of (A) **G1-H$_3$·3PF$_6$**, (B) neutral **G1**, (C) methylated **Me$_6$G2-H$_3$·9PF$_6$** and (D) methylated and deprotonated **Me$_6$G1-6PF$_6$**.

The ^{1}H NMR spectra of **G1-H$_3$·3PF$_6$** were clearly identified (Fig. 2A), dibenzylammonium (DBA) H$_e$ and H$_k$ shared an identical chemical shift at δ = 4.54 ppm, and the chemical shift at δ = 4.42 ppm was

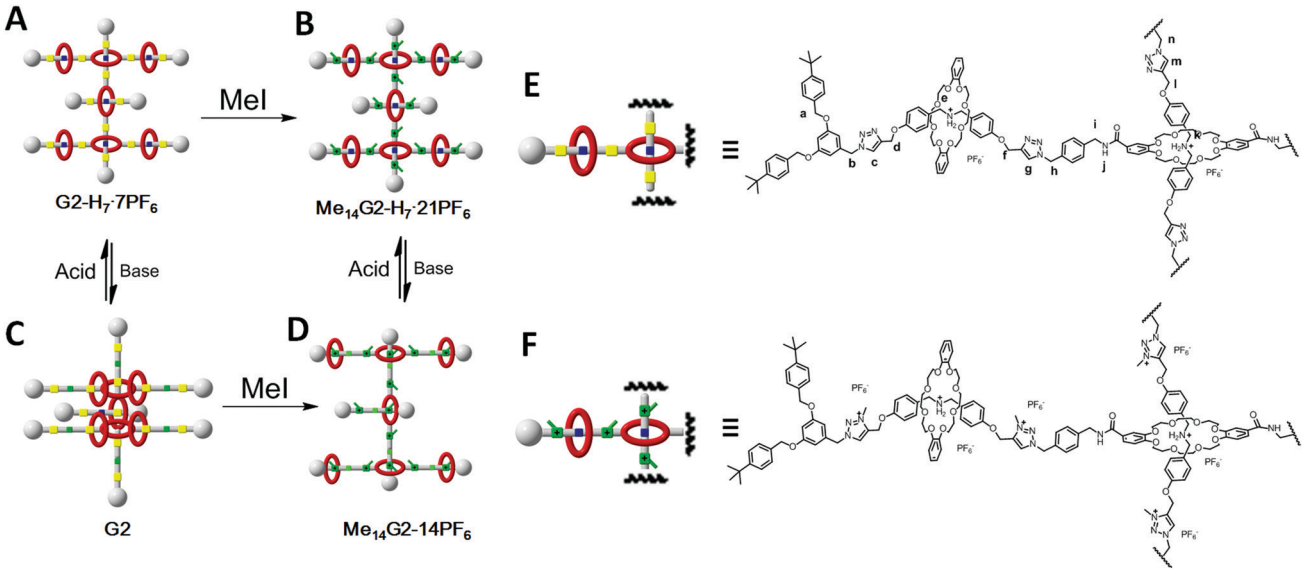

Fig. 1 Graphical representation and partial structural formula of **G2** rotaxane dendrimers.

attributed to the protons H_i near the amide. Three triazole peaks were located in the downfield region, corresponding to the three sets of triazole. From the ^{1}H NMR spectrum of **G2-H$_7$·7PF$_6$**, the peak broadening phenomenon was observed because of more repeating units (ESI,† Fig. S7). Nonetheless, **G1** and **G2** type III-C RDs shared a very similar pattern in the ^{1}H NMR spectrum with reasonable peak integration, indicating the successful synthesis of **G1-H$_3$·3PF$_6$** and **G2-H$_7$·7PF$_6$**.

Both **G1-H$_3$·3PF$_6$** and **G2-H$_7$·7PF$_6$** were subjected to methylation to methylate all the triazole units into the *N*-methyltriazolium (MTA) ion. The total number of triazole units was 6 in **G1** and 14 in **G2**. After methylation, methylated **G1** [4]rotaxane dendrimers (**Me$_6$G1-H$_3$·9PF$_6$**) carrying 9^+ charges and methylated **G2** [8]rotaxane dendrimers (**Me$_{14}$G2-H$_7$·21PF$_6$**) became the second most densely charged MIMs[16] on record carrying 21^+ charges.

The successful synthesis of all the type III-C RDs was further confirmed by high resolution electrospray-ionization mass spectrometry (HR ESI-MS). $[M\text{-}3PF_6]^{3+}$ species was observed in **G1-H$_3$·3PF$_6$**. In **G2-H$_7$·7PF$_6$** (ESI,† Fig. S93), two ion species representing $[M\text{-}7PF_6]^{7+}$ and $[M\text{-}6PF_6]^{7+}$ with *m*/*z* 1439.1611 and *m*/*z* 1703.0207 were found and are consistent with the theoretical value, implying that all the targeted type III-C RDs were successfully synthesized. The mass spectrum of **Me$_6$G1-H$_3$·9PF$_6$** (ESI,† Fig. S94) showed peaks at *m*/*z* 570.0549, 693.0532 and 832.7225 corresponding to the species of $[M\text{-}9PF_6\text{-}H]^{7+}$, $[M\text{-}7PF_6]^{7+}$ and $[M\text{–}6PF_6]^{6+}$, respectively. In the mass spectrum of **Me$_{14}$G2-H$_7$·21PF$_6$** (ESI,† Fig. S95), peaks at *m*/*z* 1520.9983, 1335.8846, 1187.7024, 1066.5527, and 965.6718 refer to the species of losing eight to twelve PF_6^- counterions. The ESI-MS evidence further confirmed that all triazoles inside the RDs were exclusively methylated.

After we confirmed the chemical synthesis, we explored the switching properties of type III-C RDs. The most interesting properties of type III-C RDs are the acid–base responsive globular switching (Fig. 1). The deprotonation of RDs was performed with BEMP resin. After deprotonation, significant NMR peak shifting was observed in all RD spectra. The methylated RDs (**Me$_6$G1-H$_3$·9PF$_6$** and **Me$_{14}$G2-H$_7$·21PF$_6$**) exhibited a different switching process in comparison to the ones without methylation. Interestingly, in the non-methylated RDs (**G1-H$_3$·3PF$_6$** and **G2-H$_7$·7PF$_6$**), the macrocycles at the periphery moved toward the amide[17] instead of the triazole unit, and only the core macrocycle oscillated between triazoles. By taking the neutral **G1** [4]rotaxane dendrimers (**G1**) as an example (Fig. 2A and B), after deprotonation, H_e and H_k shifted upfield significantly ($\Delta\delta H_{e,k}$ = −0.84 ppm), proving that the macrocycles were not located at the amine groups. In contrast, H_i experienced a downfield shift ($\Delta\delta H_i$ = 0.32 ppm), attributed to the oxygen of DB24C8 interacting with the amide protons through hydrogen bonding. In the downfield region, only the triazole protons at the core H_m shifted as two sets of resonances, by shuttling between two triazoles, and the shuttling was slow on the NMR timescale. The chemical shift of the other two triazole protons H_c and H_g was similar to that in the initial state. Also, similar chemical shifts were observed in deprotonated neutral **G2** [8]rotaxane dendrimers (**G2**) (ESI,† Fig. S8), revealing that the molecular shuttling process occurred after the deprotonation.

As expected, if RDs were methylated, a distinct shuttling process was exhibited. After the methylation (Fig. 1), all triazoles turned to MTA, a well-known secondary station for DB24C8.[17] Deprotonation of **Me$_6$G1-H$_3$·9PF$_6$** (Fig. 2C and D) led to DBA protons H_e and H_k shifting upfield ($\Delta\delta H_{e,k}$ = −0.86 ppm), and all the MTA protons H_c, H_m, and H_g shifted as two sets of resonances, revealing that the macrocycles were oscillating between two equal MTA and slow on the NMR time-scale.[18] The methyl protons of MTA shifted dramatically, due to the shielding effect by the cavity of aromatic macrocycles. The protons adjacent to amide H_i were not shifted implying that the macrocycles did not move to the amide unit. In **Me$_{14}$G2-14PF$_6$** (ESI,† Fig. S9), very similar chemical shifts can be detected, except for the MTA protons that shifted as one set of peaks. **G1**, **G2** and **Me$_6$G1-6PF$_6$**, **Me$_{14}$G2-14PF$_6$** exhibited distinct switching behaviours compared to their initial compounds. In addition, all RDs can be restored to their initial structures with at least 5 acid–base switching cycles, showing that the RDs were capable of multiple pH switching cycles without degradation (ESI,† Fig. S18–S25).

Unlike our reported type III-B RDs, dual (expansion and contraction) size modulation of type III-C RDs was achieved. Based on the NMR result, supposedly, the initial RDs will be contracted after deprotonation, whereas the size of the methylated RDs will be slightly expanded. We then analyzed the morphology and size changes of the RDs with atomic force microscopy (AFM). The AFM analysis revealed that all the RDs were nearly spherical in morphology and monodispersed when they were deposited on the mica/silicon wafer surface. **G1-H$_3$·3PF$_6$** (∼1.50 nm) and **G1** (∼1.51 nm) showed a similar height (Fig. 3A and B), while the height of **Me$_6$G1-6PF$_6$** (∼1.96 nm) was slightly greater than that of **Me$_6$G1-H$_3$·9PF$_6$** (∼2.11 nm) (Fig. 3C and D). In **G2** RDs, obvious height differences were observed. After the deprotonation of **G2-H$_7$·7PF$_6$** to **G2**, contraction was observed (Fig. 3E and F). The height decreased by about 21% from 5.06 ± 0.07 nm to 4.10 ± 0.06 nm because the mechanical bonds squeeze into the core after the deprotonation (Fig. 1C), whereas in **Me$_{14}$G2-H$_7$·21PF$_6$**,

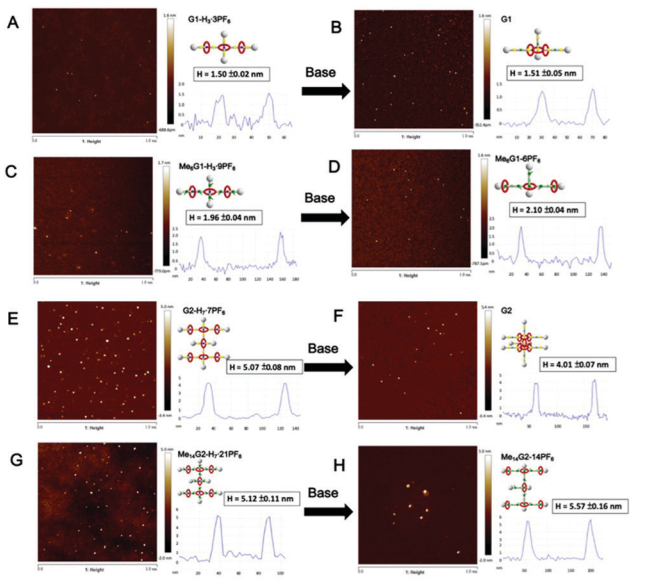

Fig. 3 AFM images of type III-C rotaxane dendrimers on the mica surface (A–F) (1 μm × 1 μm) or the silicon surface (G and H) (1 μm × 1 μm) and the height profiles.

the removal of all protons leads to the oscillation of all mechanical bonds between MTA and causes extension (Fig. 1D). The height of $\mathbf{Me_{14}G2\text{-}H_7{\cdot}21PF_6}$ was increased by about 8% from 5.11 ± 0.11 nm to 5.58 ± 0.16 nm (Fig. 3G and H). The dynamic light scattering (DLS) measurement was in agreement with AFM, supporting that the size modulation was achieved after acid/base treatment (ESI,† Fig. S27 and S28).

The neutral **G1** and **G2** were able to bind with guest molecules through electrostatic interaction and hydrophobic interaction.[9] Two small molecular weight drug molecules, chlorambucil and lithocholic acid, were separately used for the binding study. The ^{1}H NMR titration results (ESI,† Fig. S26–S29) showed that **G1** was able to bind with two chlorambucil or three lithocholic acid molecules out of its three DBA sites, while **G2** was capable of binding with six chlorambucil or seven lithocholic acid molecules out of its seven DBA sites.

Since type III-C RDs are not fluorescent in nature but thanks to its monodispersity, we finally investigated the inter-organ distribution of RDs in C57BL/6J mice with MALDI-TOF MS (Fig. 4 and ESI,† Fig. S34–S47). In both **G1** and **G2**, the accumulation in the spleen and liver was higher than in other organs, implying that the highly lipophilic **G1** and **G2** were mainly retained in the reticuloendothelial system enriched organs (Fig. 4). The amount of **G1** and **G2** in each organ after administration was increased gradually from 12 h to 24 h, and started to decrease from 36 h to 48 h due to excretion from organs. Only a trace amount of RDs was found in the spleen and none was detectable in other organs after 48 h, suggesting that the retention-time of RDs in the mice was about 48 h and they were excreted from the organs. Moreover, a fragment or its metabolite ion cannot be observed in the spectra (12 h to 48 h) indicating that both **G1** and **G2** were stable in a physiological environment and did not undergo degradation *in vivo*.

In conclusion, new type III-C RDs were successfully synthesized and characterized by various spectroscopic and microscopic techniques. Dual switching processes of **G1**/**G2** and methylated **G1**/**G2** rotaxane dendrimers were demonstrated by NMR spectroscopy, and AFM and DLS analyses. The morphology of type III-C rotaxane dendrimers tends to expand in an acidic and contract in a basic environment, while methylated rotaxane dendrimers tend to expand under basic conditions and contract under acidic conditions. These results of molecular "breathing" reveal that both non-methylated and methylated rotaxane dendrimers could be potentially applicable in binding acidic or basic drugs for actively pH-controlled drug release. Chlorambucil and lithocholic acid were capable of binding with the deprotonated **G1** and **G2**. For the first time, MALDI-TOF MS has been used to investigate the *in vivo* distribution of label-free, monodispersed type III-C rotaxane dendrimers as a potential cargo carrier. The *in vivo* experiment indicated that **G1**/**G2** tend to accumulate and remain in the reticuloendothelial system enriched spleen and liver. This study has provided a new analytical method for evaluating label-free dendrimers, dendritic materials and MIMs before biomedical applications and clinical trials. Drug delivery and more biological experiments are currently underway in our laboratory.

We acknowledge the financial support from The State Key Laboratory of Environmental and Biological Analysis, The Interdisciplinary Research Clusters (IRCS/17-18/03) and The President's Award for Outstanding Performance in Research Supervision to K. C.-F. L. from The Hong Kong Baptist University. We also acknowledge Mr David T.-W. Chik for the helpful discussion on the MALDI experiment. We acknowledge the discussions with Professor Sir Fraser Stoddart.

Conflicts of interest

There are no conflicts to declare.

Notes and references

1 J. W. Lee and K. Kim, *Top. Curr. Chem.*, 2003, **228**, 111.
2 C. J. Bruns and J. F. Stoddart, *The Nature of the Mechanical Bond: From Molecules to Machines*, Wiley, 2017.
3 K. C.-F. Leung and K.-N. Lau, *Polym. Chem.*, 2010, **1**, 988.
4 C.-S. Kwan, A. S. C. Chan and K. C.-F. Leung, *Org. Lett.*, 2016, **18**, 976.
5 A. M. Elizarov, S.-H. Chiu and J. F. Stoddart, *J. Org. Chem.*, 2002, **67**, 9175.
6 Y. Takashima, Y. Hayashi, M. Osaki, F. Kaneko, H. Yamaguchi and A. Harada, *Macromolecules*, 2018, **51**, 4688.
7 C. Cheng, P. R. McGonigal, S. T. Schneebeli, H. Li, N. A. Vermeulen, C. Ke and J. F. Stoddart, *Nat. Nanotechnol.*, 2015, **10**, 547.
8 Y. Wang, T. Cheng, J. Sun, Z. Liu, M. Frasconi, W. A. Goddard and J. F. Stoddart, *J. Am. Chem. Soc.*, 2018, **140**, 13827.
9 C.-S. Kwan, R. Zhao, M. A. Van Hove, Z. Cai and K. C.-F. Leung, *Nat. Commun.*, 2018, **9**, 497.
10 W. K. W. Ho, S.-F. Lee, C.-H. Wong, X.-M. Zhu, C.-S. Kwan, C.-P. Chak, P. M. Mendes, C. H. K. Cheng and K. C.-F. Leung, *Chem. Commun.*, 2013, **49**, 10781.
11 W. Wang, L.-J. Chen, X.-Q. Wang, B. Sun, X. Li, Y. Zhang, J. Shi, Y. Yu, L. Zhang, M. Liu and H.-B. Yang, *Proc. Natl. Acad. Sci. U. S. A.*, 2015, **112**, 5597.
12 Y.-X. Wang, Q.-F. Zhou, L.-J. Chen, L. Xu, C.-H. Wang, X. Li and H.-B. Yang, *Chem. Commun.*, 2018, **54**, 2224.
13 X.-Q. Wang, W. Wang, W.-J. Li, L.-J. Chen, R. Yao, G.-Q. Yin, Y.-X. Wang, Y. Zhang, J. Huang, H. Tan, Y. Yu, X. Li, L. Xu and H.-B. Yang, *Nat. Commun.*, 2018, **9**, 3190.
14 Z. Li, G. Liu, W. Xue, D. Wu, Y.-W. Yang, J. Wu, S. H. Liu, J. Yoon and J. Yin, *J. Org. Chem.*, 2013, **78**, 11560.
15 D. A. Tomalia and J. M. J. Fréchet, *J. Polym. Sci., Part A: Polym. Chem.*, 2002, **40**, 2719.
16 M. T. Nguyen, D. P. Ferris, C. Pezzato, Y. Wang and J. F. Stoddart, *Chem*, 2018, **4**, 2329.
17 B. Riss-Yaw, J. Morin, C. Clavel and F. Coutrot, *Molecules*, 2017, **22**, 2017.
18 Z. Meng, J.-F. Xiang and C.-F. Chen, *J. Am. Chem. Soc.*, 2016, **138**, 5652.

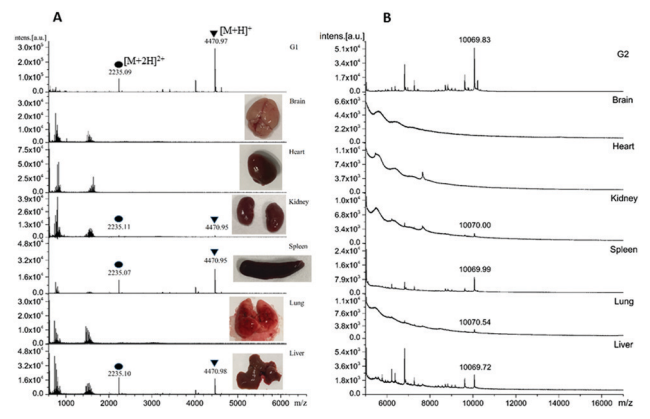

Fig. 4 **G1** MALDI-MS spectral (24 h) profiles (A) of the standard (top) and organs obtained from **G1** intraperitoneally injected mice. The single charged (▼) and double charged (•) ion species were labelled. **G2** MALDI-MS spectral (24 h) profiles (B) of the standard (top) and organs obtained from **G2** intraperitoneally injected mice.